

MODELS OF PARTICLE REINFORCED NONLINEAR-VISCOUS COMPOSITE

By V. S. Deshpande¹ and D. Cebon²

ABSTRACT: Two new models are described for a composite consisting of a nonlinear viscous matrix reinforced by rigid particulate inclusions: (1) An analytical plane strain solution for a uniform regular array of rigid hexagonal particles separated by a nonlinear viscous material; and (2) a numerical upper-bound solution using Hashin's composite sphere model for a composite consisting of rigid inclusions in a nonlinear viscous matrix. Suquet's closed-form solution for the nonlinear composite, obtained by transforming Hashin's linear solution, is also examined. Predictions of all models are compared with experimental measurements from uniaxial compression tests on composites consisting of bitumen reinforced with various volume fractions of aggregate.

INTRODUCTION

Bituminous mixes (or asphalts) used in "flexible" pavements are complex materials consisting of a high volume fraction of graded aggregate, air voids, and bitumen. The research described in this paper is part of a larger project to understand the deformation behavior of asphalt road surfaces. As a first step toward understanding the deformation of real mixes, the behavior of idealized mixes (with simple microstructures) is investigated here.

Cheung and Cebon (1996a) found that for most practical operating conditions bitumen is a nonlinear viscous material with a constitutive law (see the section entitled Experiments on Idealized Bituminous Mixes for further details)

$$\frac{\dot{\epsilon}_{ij}}{\dot{\epsilon}_0} = \frac{3}{2} \left(\frac{\sigma_e}{\sigma_0} \right)^{n-1} \frac{\Sigma'_{ij}}{\sigma_0} \quad (1)$$

where $\dot{\epsilon}_0$ = reference strain rate; σ_0 = reference stress; σ_e = von Mises equivalent stress; Σ'_{ij} = deviatoric stress tensor; $\dot{\epsilon}_{ij}$ = strain rate tensor; and n = stress sensitivity (power law index).

Cheung and Cebon measured the properties of a 50 pen bitumen and found it to have a power law index of $n = 2.3$. [Pen is a standard index that describes the penetration characteristics of bitumen. For details see *Shell bitumen handbook* (Whiteoak 1990).] Because the aggregate particles in the asphalt are very stiff relative to the bitumen matrix [at 20°C the rate of Young's modulus of the aggregate to the initial modulus of bitumen is ≈ 100 (Cheung 1995)], asphalt can be modeled as a nonlinear viscous composite, with bitumen reinforced by a high volume fraction of rigid particles.

Work on modeling the deformation behavior of nonlinear viscous materials reinforced by rigid inclusions was reviewed by Deshpande (1997), who found that existing models fall into the following three categories:

1. Homogenization formulas for the properties of periodic composites.
2. Estimates for the effective properties of ad hoc models of composites.
3. Variational boundaries for the properties of random composites.

The homogenization approach most often involves construc-

tion of a unit cell and solution of the resultant boundary value problem by finite-element (FE) analysis. The ad hoc models [e.g., Duva's (1984) differential self-consistent analysis] generate approximate relationships for nondilute composites based upon known results for dilute composites. An FE calculation for rigid spherical inclusions in a nonlinear viscous matrix was carried out by Bao et al. (1991). They found that their results were very similar to Duva's differential self-consistent estimate. Also, Deshpande (1995) showed that most upper and lower variational bounds for the properties of asphaltic composites are generally too far apart to be of any practical use.

In this paper two models are considered for the deformation of idealized asphalt mixes (i.e., bitumen with high volume fractions of particulate inclusions):

1. A uniform array of rigid hexagonal particles separated by a nonlinear viscous matrix.
2. An upper-bound solution using Hashin's (1962) composite sphere model for a composite consisting of rigid inclusions randomly distributed in a nonlinear viscous matrix.

The theoretical results are compared with uniaxial compression tests on idealized bitumen composites (i.e., bitumen reinforced with uniformly graded sand or single sized glass beads) previously performed by Deshpande (1995).

HEXAGONAL ARRAY MODEL

In this section a plane strain solution for a nonlinear viscous material reinforced by a regular array of rigid hexagonal particles is presented. Hexagonal particles were chosen because

1. Hexagons can be arranged to give a high volume fraction of inclusions (more than that from a packing of single sized spheres).
2. The parallel "flat plate" contacts separating the hexagons can be analyzed easily and represent a limiting case deformation mechanism, consisting of flow without damage or void growth.

Drucker (1964) performed a similar analysis for a matrix phase consisting of an ideally plastic or a linear viscous material. Bao et al. (1991) repeated this analysis. The general nonlinear viscous solution presented here agrees with Drucker's solution in the two limiting cases.

Compatibility

The microstructure to be analyzed is shown in Fig. 1. An infinite, regular, two-dimensional (2D) array of rigid hexagonal prisms with side $2L$, separated by continuous thin films of a nonlinear viscous material of thickness $2h_1$ or $2h_2$, is subjected to remote biaxial stresses Σ_1^{∞} and Σ_2^{∞} . The rectangle

¹Res. Assoc., Dept. of Engrg., Univ. of Cambridge, Trumpington St., Cambridge, CB2 1PZ, U.K.

²Reader, Dept. of Engrg., Univ. of Cambridge, Trumpington St., Cambridge, CB2 1PZ, U.K.

Note. Associate Editor: Sunil Saigal. Discussion open until August 1, 1999. To extend the closing date one month, a written request must be filed with the ASCE Manager of Journals. The manuscript for this paper was submitted for review and possible publication on March 26, 1997. This paper is part of the *Journal of Engineering Mechanics*, Vol. 125, No. 3, March, 1999. ©ASCE, ISSN 0733-9399/99/0003-0255-0262/\$8.00 + \$.50 per page. Paper No. 15440.

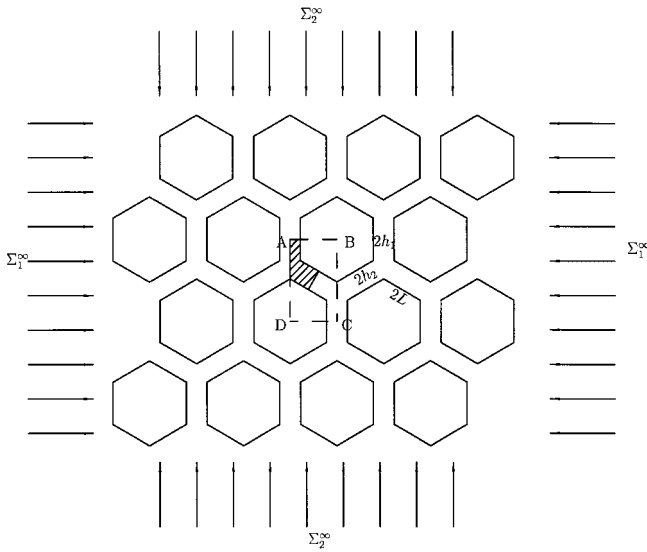


FIG. 1. Regular 2D Array of Hexagonal Prisms Subjected to Remote Stresses Σ_1^∞ and Σ_2^∞

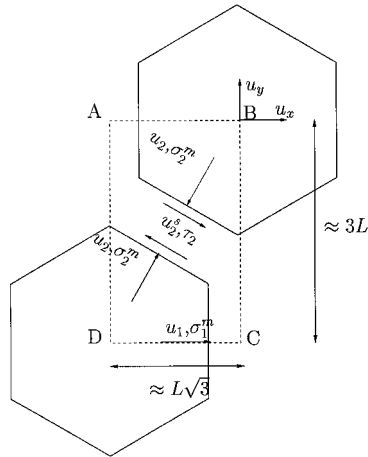


FIG. 2. Repeating Unit of Fig. 1 Shown with Local Boundary Velocities and Stresses

ABCD represents a unit cell, which is chosen such that the sides AB, BC, CD, and DA are all axes of symmetry. A consequence of this is that the hexagonal prisms are not able to rotate, and as a result the film thickness in each parallel channel remains uniform as the array deforms. Fig. 2 shows the velocities associated with the boundaries. u_x and u_y are the relative horizontal and vertical velocities of the two prisms, respectively (i.e., the motion of point B relative to fixed point D). These can be related to the velocity components u_1 and u_2 (u_1 is the velocity of C relative to D and u_2 is the relative normal velocity of the diagonal planes of the hexagons) by

$$u_x = u_1 \quad (2)$$

$$u_y = \frac{2u_2 - u_1}{\sqrt{3}} \quad (3)$$

For thin films the resulting remote strain rates in the horizontal and vertical directions are

$$\dot{E}_{11}^\infty = \frac{u_1}{L\sqrt{3}} \quad (4)$$

$$\dot{E}_{22}^\infty = \frac{2}{3} \left(\frac{u_2 - u_1/2}{L\sqrt{3}} \right) \quad (5)$$

The volume of the shaded region in Fig. 1 is given by

$$V \approx Lh_1 + 2Lh_2 \quad (6)$$

where higher-order terms in h have been neglected because the films are thin. From symmetry considerations it can be seen that there is no flow out of this volume. Because the matrix material is incompressible [according to the constitutive law given by (1)]

$$\dot{V} = L(\dot{h}_1 + 2\dot{h}_2) = 0 \quad (7)$$

This constrains the relationship between the two strain rates. Furthermore, the velocities u_1 and u_2 are related simply to the rates of change of film thicknesses h_1 and h_2 by

$$\dot{h}_1 = u_1 \quad (8)$$

$$2\dot{h}_2 = u_2 \quad (9)$$

Hence from (5) and (7)

$$\dot{h}_2 = \frac{L\sqrt{3}}{2} \dot{E}_{22}^\infty \quad (10)$$

$$\dot{h}_1 = -L\sqrt{3} \dot{E}_{22}^\infty \quad (11)$$

Equilibrium

Because the films are thin, the shear forces in the bitumen films can be assumed to be much smaller than the normal forces [see Cheung and Cebon 1996b] for details of thin film behavior]. Therefore the hexagonal prisms can be assumed to be free to slide. Denoting σ_1^m and σ_2^m as the mean stresses transmitted across the vertical and diagonal boundaries, respectively (Fig. 2), equilibrium requires that (Cocks and Ashby 1982)

$$\sigma_1^m = \frac{1}{2} (3\Sigma_1^\infty - \Sigma_2^\infty) \quad (12)$$

$$\sigma_2^m = \Sigma_2^\infty \quad (13)$$

It should be noted that the stress-concentration at the corners has been ignored.

Governing Equations for Thin Film Behavior

Cheung and Cebon (1996b) showed that deformation characteristics of a thin film of bitumen under plane strain conditions is given by

$$\frac{\sigma_n + P_0}{\sigma_0} = \left(\frac{n}{2n+1} \right) (n+2)^{1/n} \left(\frac{A}{\sqrt{3}} \right)^{(n+1)/n} \left(\frac{|\dot{h}|/h}{\dot{\epsilon}_0} \right)^{1/n} \text{sign}(\dot{h}) \quad (14)$$

where σ_n = normal stress; P_0 = pressure at the ends of the contact film; A = aspect ratio of the contact = L/h ; and h = half film thickness. The sign convention used here is tension +ve, and compression -ve.

FE analysis of the thin film compression of bitumen performed by Cheung and Cebon showed that the analytical solution for the thin film behavior given earlier is accurate for $A \geq 5$. For aspect ratios < 5 the one-dimensional (1D) flow assumption made in the analytical solution is not satisfactory and the FE analysis predicts that the films are stiffer than that calculated from (14).

The relationship between the volume fraction of hexagons f and film aspect ratio A for an initially regular array is

$$A = \frac{1}{\sqrt{3}} \left(\frac{\sqrt{f}}{1 - \sqrt{f}} \right) \quad (15)$$

For an array consisting of, for example, 64% by volume of hexagonal prisms, the aspect ratio $A \approx 2.3$ [64% by volume

corresponds to the dense random packing density of single size spheres (Scott and Kilgour 1969)]. A correction factor obtained from the FE analysis (Cheung and Cebon 1996b) can be added to correct (14) in such cases [a graph showing this correction factor versus aspect ratio is given in Cheung and Cebon (1996b)].

Overall Constitutive Law

There are two typical contacts in the array, namely, those represented by the vertical and diagonal boundaries in Fig. 2. Substituting the stress at these contacts [(12) and (13)] into the deformation law given by (14) and subtracting the resulting equations to eliminate P_0 (the pressure at the vertices between the hexagons) gives

$$\frac{3}{2} \left(\frac{\Sigma_1^\infty - \Sigma_2^\infty}{\sigma_0} \right) = \left(\frac{n}{2n+1} \right) (n+2)^{1/n} \left(\frac{1}{\sqrt{3}} \right)^{(n+1)/n} \cdot \left[\left(\frac{L}{h_1} \right)^{(n+1)/n} \left(\frac{|\dot{h}_1|}{h_1} \right)^{1/n} \text{sign}(\dot{h}_1) - \left(\frac{L}{h_2} \right)^{(n+1)/n} \left(\frac{|\dot{h}_2|}{h_2} \right)^{1/n} \text{sign}(\dot{h}_2) \right] \left(\frac{1}{\dot{\epsilon}_0} \right)^{1/n} \quad (16)$$

It should be noted that this ignores most of the complexity of the flow at the channel intersections.

Eliminating h_1 and h_2 using (10) and (11) gives

$$\frac{\Sigma_2^\infty - \Sigma_1^\infty}{\sigma_0} = \left(\frac{2n}{3(2n+1)} \right) (n+2)^{1/n} \left(\frac{1}{\sqrt{3}} \right) \cdot \left[\left(\frac{L}{h_1} \right)^{(n+2)/n} + \left(\frac{1}{2} \right)^{1/n} \left(\frac{L}{h_2} \right)^{(n+2)/n} \right] \left(\frac{|\dot{E}_{22}^\infty|}{\dot{\epsilon}_0} \right)^{1/n} \text{sign}(\dot{E}_{22}^\infty) \quad (17)$$

It should be noted that $\Sigma_2^\infty - \Sigma_1^\infty$ will always have the same sign as \dot{E}_{22}^∞ and vice versa. The constitutive law can then be written as

$$\frac{\dot{E}_{22}^\infty}{\dot{\epsilon}_0} = \frac{1}{S} \left(\frac{|\Sigma|}{\sigma_0} \right)^n \text{sign}(\Sigma) \quad (18)$$

where $\Sigma = \Sigma_2^\infty - \Sigma_1^\infty =$ measure of the deviatoric stress; and

$$S = \left(\frac{2n}{3(2n+1)} \right)^n (n+2) \left(\frac{1}{\sqrt{3}} \right)^n \cdot \left[\left(\frac{L}{h_1} \right)^{(n+2)/n} + \left(\frac{1}{2} \right)^{1/n} \left(\frac{L}{h_2} \right)^{(n+2)/n} \right]^n \quad (19)$$

The parameter S is known as the ‘‘stiffening effect.’’ In the case of uniaxial loading (i.e., either $\Sigma_2^\infty = 0$ or $\Sigma_1^\infty = 0$), S is the ratio of the steady-state strain rate of the matrix material (pure bitumen) to the strain rate of the array, under the same uniaxial stress. It can be seen from (19) that the value of S predicted by this analysis is a function of the microstructural parameters only and not a function of the stress state.

Evolution of Constitutive Law

An approximate large strain solution for the deformation of the array is described in this section. Assume that the array starts from an initially regular geometry with $h_1 = h_2 = h_0$ (i.e., $L/h_1 = L/h_2 = L/h_0 = A_0$, where A_0 is the initial aspect ratio). As the array deforms, the film thickness h_1 and h_2 change, and hence the constitutive law varies with strain.

The microstructural parameter h_2 varies as

$$\frac{L}{h_2} = \frac{L}{h_0 + \int_0^t \dot{h}_2 dt} \quad (20)$$

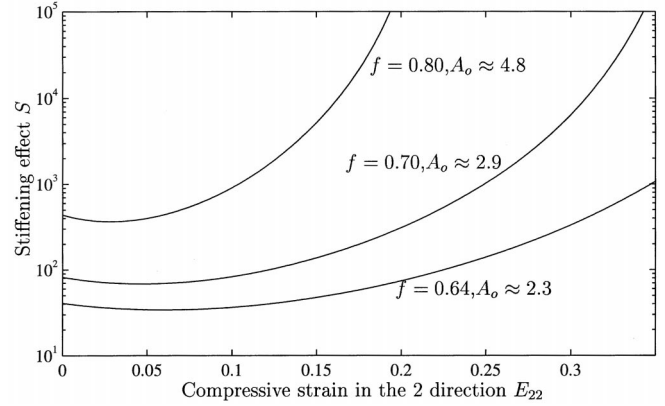


FIG. 3. Variation of Stiffening Effect S with Strain in 2-Direction ($n = 2.3$)

Substituting for h_2 from (10) gives

$$\frac{L}{h_2} = \frac{A_0}{1 + \frac{\sqrt{3}A_0}{2} \int_0^t \dot{E}_{22}^\infty dt} = \frac{A_0}{1 + \frac{\sqrt{3}}{2} A_0 E_{22}^\infty} \quad (21)$$

Because the matrix material is incompressible, (6) can be rewritten as

$$\frac{h_1}{L} = \frac{3}{A_0} - \frac{2h_2}{L} \quad (22)$$

Eqs. (18), (19), and (22) can be used to predict the evolution of the constitutive law with compressive strain in the 2-direction for the array of hexagonal prisms [it is assumed that the equilibrium conditions given by (12) and (13) still hold]. Fig. 3 shows the variation of the stiffening effect S with strain for various volume fractions (or initial aspect ratios A_0) of hexagonal prisms in a bitumen matrix with $n = 2.3$. It can be seen that, for compression in the 2-direction, initially there is a small drop in stiffness of the array. This is because as h_1 increases the pressure at the vertices P_0 decreases. The mix then deforms at essentially a constant rate (stiffening effect) until the strains reach ~ 0.1 (10%). The stiffening effect then increases rapidly (deformation rate decreases) as the diagonal films become very thin ($h_2 \rightarrow 0$) and very stiff ($\sigma_2^m \rightarrow \infty$).

COMPOSITE SPHERE MODEL

In the previous section a composite with a particular uniform microstructure was analyzed. In most realistic cases for particulate composites, the microstructure is random. Hence only bounds on the properties of the composite can be obtained using the limited information available about the composite, such as the volume fraction of the phases, etc. In several cases of practical importance, inclusions of one phase (e.g., Phase 1) are embedded in another phase (Phase 2). A model morphology accounting for this information was constructed by Hashin (1962). It consists of an assemblage of composite spheres. In this section an upper-bound solution is derived using Hashin’s model. A numerical calculation technique is employed to calculate the stiffening effect for a composite consisting of rigid inclusions in a nonlinear viscous matrix.

An approximate extension of Hashin’s lower bound was given by Suquet (1993) for rigid inclusions in a nonlinear viscous matrix. This bound was found to agree well with experimental data only for a low volume fraction of rigid inclusions. Because a model is being developed in this paper for asphalt that contains ≈ 75 – 85% aggregate, only Hashin’s upper bound is considered.

Hashin's Composite Sphere Model

Hashin (1962) described a composite consisting of a matrix with embedded inclusions by the composite sphere assemblage shown schematically in Fig. 4. The broken curves, drawn in Fig. 4, define the region of the matrix phase associated with each particle. The ratio a/b is taken to be constant for each composite sphere. Consequently a gradation of particle sizes is required to provide a space-filling configuration.

The unit cell of this model is the composite sphere shown in Fig. 5. It is defined to have $(a/b)^3 = f =$ volume fraction of the inclusion phase. Hashin (1962) showed that upper and lower bounds on the elastic modulus of the composite can be obtained by applying either uniform displacement or uniform stress fields, respectively, on the outer surface A_R of the composite sphere. Although he obtained the exact solution for the bulk modulus of a two-phase linear composite (i.e., the bounds coincided), it was only possible to get bounds for the shear modulus.

Nonlinear Composite Sphere Model

In this section Hashin's composite sphere upper bound for the "shear modulus" is developed for a composite consisting of a nonlinear viscous matrix reinforced by rigid inclusions. The "bulk modulus" is trivial (∞) as both phases are incompressible.

Analytical solutions for the velocity field in a composite sphere consisting of a rigid sphere surrounded by a nonlinear viscous material, subject to uniform surface shear straining, do not exist. Hence a numerical solution using a technique suggested by Budiansky et al. (1982) is used here.

Consider a rigid particle of radius a in an incompressible

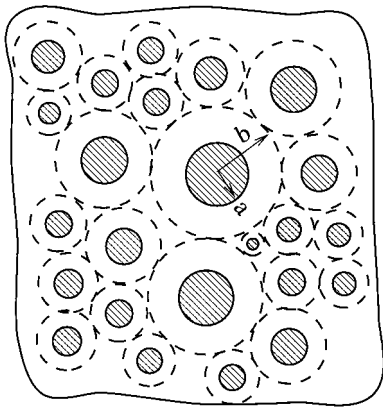


FIG. 4. Hashin's Assemblage of Composite Spheres

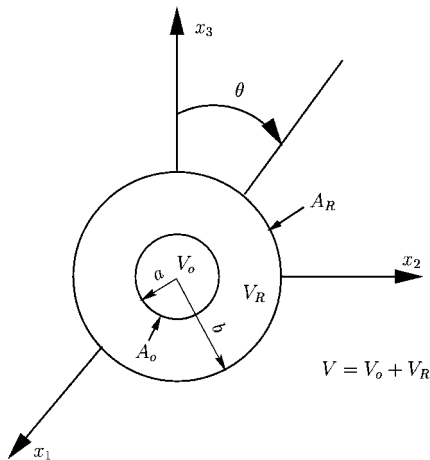


FIG. 5. Composite Sphere

nonlinear viscous matrix of radius b as illustrated in Fig. 5. The outer surface A_R is subjected to uniform straining $\mathbf{v}_i = \dot{\mathbf{E}}_{ij}x_j$, where \mathbf{v}_i is the velocity vector; and $\dot{\mathbf{E}}_{ij}$ the macroscopic strain rate tensor. Because the body is incompressible, only axisymmetric straining can be considered without the loss of generality. Hence the body is subjected to a distortional strain rate given by

$$\dot{\mathbf{E}} = \frac{2}{3} (\dot{E}_{33} - \dot{E}_{11}) \quad (23)$$

where $\dot{E}_{33} =$ macroscopic axial strain rate; and $\dot{E}_{11} =$ macroscopic radial strain rate.

The minimum principle for velocities stated by Hill (1956) is used to find approximate Rayleigh-Ritz solutions. The velocities \mathbf{v}_i minimize the stress potential Φ given by

$$\Phi = \frac{1}{|V|} \int_{V_R} W(\dot{\mathbf{E}}) dV \quad (24)$$

where

$$W(\dot{\mathbf{E}}) = \int_0^{\dot{\mathbf{E}}} \sigma_{ij} d\epsilon_{ij} = \frac{n}{n+1} \sigma_0 \dot{\epsilon}_0 \left(\frac{\dot{\epsilon}_e}{\dot{\epsilon}_0} \right)^{(n+1)/n} \quad (25)$$

and

$$\dot{\epsilon}_e = \left(\frac{2}{3} \dot{\epsilon}_{ij} \dot{\epsilon}_{ij} \right)^{1/2} \quad (26)$$

It should be noted that the repeated indices denote summation (tensor notation).

The usual admissibility conditions

$$\mathbf{v}_{i,i} = 0; \quad \dot{\epsilon}_{ij} = \frac{1}{2} (\mathbf{v}_{i,j} + \mathbf{v}_{j,i}) \quad (27a,b)$$

are imposed. The comma denotes differentiation with respect to that variable. The stress tensor is then given by the constitutive relation

$$\Sigma_{ij} = \frac{\partial \Phi}{\partial \dot{\mathbf{E}}_{ij}} \quad (28)$$

Numerical Solution Formulation

A general representation of the incompressible, axisymmetric velocity field in spherical coordinates (r, θ, ϕ) can be written in terms of a stream function $\chi(r, \theta)$ as

$$v_r = -r^{-2} (\sin \theta)^{-1} (\chi \sin \theta)_{,\theta} \quad (29)$$

$$v_\theta = r^{-1} \chi_{,r} \quad (30)$$

where v_r and $v_\theta =$ velocities in the radial and tangential directions, respectively.

This definition of the velocity field always ensures incompressibility (i.e., $\mathbf{v}_{i,i} = 0$). For a field that is symmetric about $\theta = \pi/2$, χ can be expressed as

$$\chi(r, \theta) = \sum_{k=2,4,\dots} P_{k,\theta}(\cos \theta) f_k(r) \quad (31)$$

where $P_k(\cos \theta) =$ Legendre polynomial degree k . The unknown functions $f_k(r)$ that must be chosen to minimize Φ in (24) are approximated by a finite number of terms using

$$f_k(r) = \sum_{j=-\infty}^{\infty} A_k^{(j)} r^j \quad (32)$$

where amplitudes $A_k^{(j)}$ are to be determined in the minimization.

Love (1944), Sternberg et al. (1951), and Hashin (1962) presented the exact solution to the preceding problem for the

case when a linear elastic (or linear viscous) material surrounds the rigid inclusion. In these cases, the stream function χ has the form

$$\chi(r, \theta) = P_{2,0}(\cos \theta) \left(A_2^{(5)} r^5 + A_2^{(3)} r^3 + A_2^{(0)} + \frac{A_2^{(-2)}}{r^2} \right) \quad (33)$$

where $A_2^{(5)}, A_2^{(3)}, A_2^{(0)}, A_2^{(-2)}$ = constants, derived from the boundary conditions. The trial function $f_k(r)$ must be chosen in the current case, so that it at least incorporates this exact linear solution. Hence the minimum number of terms representing $f_k(r)$ must be

$$f_k(r) = \sum_{i=-2}^5 A_k^{(i)} r^i \quad (34)$$

From (29) and (30)

$$v_r = \sum_{k=2,4,\dots} k(k+1) P_k(\cos \theta) r^{-2} f_k(r) \quad (35)$$

$$v_\theta = \sum_{k=2,4,\dots} P_{k,\theta}(\cos \theta) r^{-1} f_{k,r}(r) \quad (36)$$

The velocity field previously given does not automatically satisfy the boundary conditions on A_0 and A_R . Hence the amplitudes $A_k^{(i)}$ are not free to take arbitrary values but are constrained at the inner and outer surfaces of the matrix such that

$$v_r = v_\theta = 0 \quad \text{at } r = a \quad \text{for all } \theta \quad (37)$$

$$\mathbf{v}_i = \dot{\mathbf{E}}_{ij} x_j \quad \text{on } A_R \quad (38)$$

For axisymmetric shear straining the boundary condition on A_R reduces to

$$v_r|_b = (3 \cos^2 \theta - 1) \dot{E} b \quad (39)$$

$$v_\theta|_b = -\frac{3}{2} \sin 2\theta \dot{E} b \quad (40)$$

Expressions for the associated strain rates are derived from the velocity field using

$$\dot{\epsilon}_r = v_{r,r}; \quad \dot{\epsilon}_\theta = r^{-1} v_{\theta,\theta} + r^{-1} v_r \quad (41a,b)$$

$$\dot{\epsilon}_\phi = -\dot{\epsilon}_r - \dot{\epsilon}_\theta; \quad \dot{\epsilon}_{r\theta} = \frac{1}{2} (r^{-1} v_{r,\theta} - r^{-1} v_{\theta,r} + v_{\theta,r}) \quad (41c,d)$$

For convenience the amplitude factors $A_k^{(i)}$ [which are chosen such that the constraints given by (37) and (38) are satisfied] are denoted collectively by $\{A\}$. Φ can then be written as

$$\Phi(\{A\}) = \frac{3n}{(n+1)} \sigma_0 \dot{\epsilon}_0 \int_{a/b}^1 \int_0^{\pi/2} \left(\frac{\dot{\epsilon}_e}{\dot{\epsilon}_0} \right)^{(n+1)/n} R^2 \sin \theta \, d\theta \, dR \quad (42)$$

where $R = r/b$.

Φ must be minimized with respect to the unknowns $\{A\}$. Substituting for $\dot{\epsilon}_e$ in terms of \dot{E} [using (26), (37), (38), and (41)] in the preceding equation, Φ_{\min} will have the form

$$\Phi_{\min} = g(n, a/b) \sigma_0 \dot{\epsilon}_0 \left(\frac{\dot{E}}{\dot{\epsilon}_0} \right)^{(n+1)/n} \quad (43)$$

where the number $g(n, a/b)$ is provided by the numerical solution. Using the constitutive relation (28), the strain rate \dot{E} is then given by

$$\dot{E} = \frac{\dot{\epsilon}_0}{\left[\left(\frac{n+1}{n} \right) g(n, a/b) \right]^n} \left(\frac{\Sigma}{\sigma_0} \right)^n \quad (44)$$

where $\Sigma = \Sigma_{33} - \Sigma_{11}$. For a homogeneous sphere consisting

of a nonlinear viscous matrix, with no inclusion, subject to the same boundary conditions (i.e., the preceding problem with $a = 0$), the strain rate will similarly be given by

$$\dot{E} = \frac{\dot{\epsilon}_0}{\left[\left(\frac{n+1}{n} \right) g(n, 0) \right]^n} \left(\frac{\Sigma}{\sigma_0} \right)^n \quad (45)$$

By comparing (44) and (45) the stiffening effect S of a particular volume fraction $f = (a/b)^3$ of rigid inclusions is then given by

$$S = \left[\frac{g(n, f)}{g(n, 0)} \right]^n \quad (46)$$

Numerical Implementation

The double integral in (42) cannot be evaluated analytically in terms of the amplitude factors except in the case when $n = 1$. Hence it was evaluated numerically using an adaptive recursive Newton-Codes eight-panel rule (Forsythe et al. 1977).

Minimization of Φ with respect to the amplitude factors $\{A\}$ was achieved by a numerically implemented quasi-Newton method (Shamo 1970). All numerical implementation was done using standard library functions in Matlab.

The choice of functions used for the representation of $\chi(r, \theta)$ included the four terms from the linear case [(33)] and was guided by the results of trial calculations aimed at reaching the minimum of Φ most efficiently. Terms were added to χ given by (33) until no further reduction in the value of Φ was observed. Fig. 6 shows results obtained by using χ given by (33) and

$$\chi(r, \theta) = P_{2,0}(\cos \theta) \left(A_2^{(5)} r^5 + A_2^{(4)} r^4 + A_2^{(3)} r^3 + A_2^{(2)} r^2 + A_1^{(4)} r + A_2^{(0)} + \frac{A_2^{(-1)}}{r} + \frac{A_2^{(-2)}}{r^2} \right) \quad (47)$$

In the case of χ given by (33), no minimization was necessary, while with χ given by (47) minimization with respect to four unconstrained amplitude factors was carried out [note that there are four linear constraints from the boundary conditions given by (37) and (38)]. In some of the exploratory calculations as many as 12 amplitude factors [$A_2^{(i)}$, where $i = -4, \dots, 7$] were used to represent $f_2(r)$. This yielded results not appreciably different from those obtained using (47). Also only the second-degree Legendre polynomial terms (P_2) were found to be important, with the terms containing P_4, P_6, \dots having little influence on the results. Thus (47) was found to

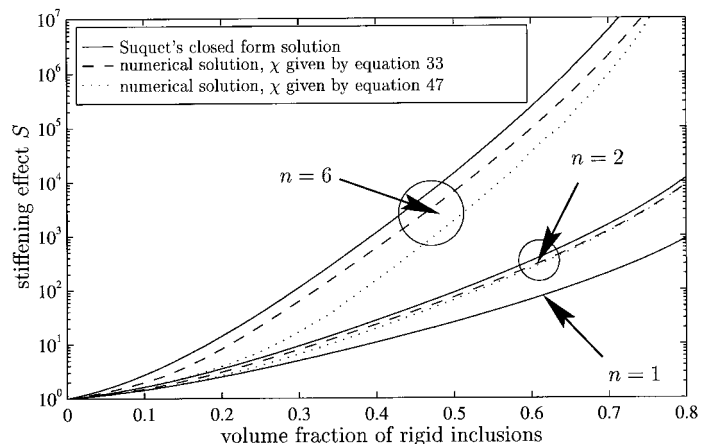


FIG. 6. Comparison between Suquet's Upper Bound and Numerically Evaluated Upper Bounds for Hashin's Composite Sphere Model

give a good representation of the stream function χ for all conditions investigated, and further results are presented only for χ as given by (47).

As a check for the numerical method the minimization procedure was carried out for the linear case ($n = 1$) with different representations for χ . It can be seen from Fig. 6 that the results coincided with Hashin's analytical solution as expected.

Comparison with Suquet's Upper Bound

Suquet (1993) proposed a method for transposing any upper-bound solution for a linear viscous composite to a corresponding upper bound for a nonlinear viscous composite with the same microstructure. For the case of a nonlinear viscous material, reinforced by rigid inclusions, Hashin's upper bound for the linear composite sphere assemblage can be transposed to the nonlinear case, to derive the stiffening effect S . This gives the closed form solution

$$S = (1 - f)^{(n+1)/2} \left[1 + f \left(\frac{2}{5} (1 - f) - \frac{f(1 - f^{2/3})^2}{-\frac{10}{21} f^{7/3} + \frac{10}{21}} \right)^{-1} \right]^{(n+1)/2} \quad (48)$$

A comparison between Suquet's analytical upper bound and the numerically evaluated upper bound for the composite sphere model is shown in Fig. 6. It can be seen from Fig. 6 that, while Suquet's linear to nonlinear transformation works well for low n , Suquet's method overestimates S appreciably at high values of n .

Most of the work done on bounding the effective properties of nonlinear composites is based on extending theories developed for linear composites. Major progress in this direction was made by extending the Hashin-Shtrikman (1962) variational structure to nonlinear problems, initiated by Willis (1983) and developed generally by Talbot and Willis (1985) and Willis (1989). Ponte Castañeda and Willis (1988), using the Talbot and Willis method, and Ponte Castañeda (1991), using another prescription, developed bounds for the effective properties of general nonlinear viscous composites. Suquet's results agree with these bounds for the special case of voids or rigid inclusions in a nonlinear viscous matrix.

A perturbation expansion by Suquet and Ponte Castañeda (1993) for weakly inhomogeneous nonlinear composites, which is exact to the second order, showed that the nonlinear bounds and estimates of the Hashin-Shtrikman type, resulting from the preceding variational procedures, are only exact to the first order. Thus, Hashin's composite sphere bound that is a second-order pattern bound (Hervé et al. 1991), when transformed to the nonlinear case using Suquet's method, is reduced to a first-order bound. [For a more detailed review see Deshpande (1997).]

EXPERIMENTS ON IDEALIZED BITUMINOUS MIXES

Deshpande (1995) carried out an extensive experimental study on the deformation behavior of idealized bituminous mixes. A brief summary of that experimental investigation is given in this section.

Pure Bitumen

Cheung and Cebon (1996a) developed mathematical models for the deformation behavior of a 50 pen bitumen over a wide range of temperatures and strain rates. For temperatures above $\approx -10^\circ\text{C}$ they found that the steady-state deformation behavior of bitumen could be described by the "modified Cross model" (Cheung and Cebon 1996a)

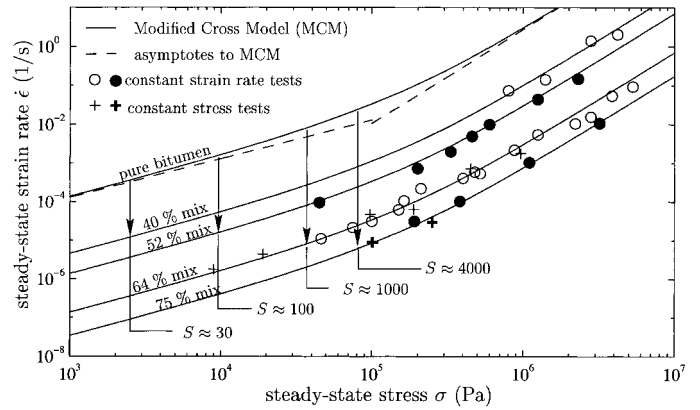


FIG. 7. Some Experimental Results from Compression Tests on Idealized Bituminous Mixes at 20°C (Deshpande 1995). Data for Mix with 40% by Volume Sand Were Corrected from Measurement Temperature of 0 to 20°C Using Eq. (50)

$$\frac{\sigma}{\sigma_0} = \frac{\dot{\epsilon}}{\dot{\epsilon}_0} \left(\frac{1}{1 + \left(\frac{\dot{\epsilon}}{\dot{\epsilon}_0} \right)^{n_c}} \right) \quad (49)$$

where n_c , σ_0 , $\dot{\epsilon}_0$ = material constants for bitumen. They also found that the temperature dependence of bitumen was activation energy controlled at low temperatures ($T < 20^\circ\text{C}$ for his bitumen) and free volume controlled at higher temperatures ($T > 20^\circ\text{C}$)

$$\frac{\dot{\epsilon}_{0c}}{\dot{\epsilon}_0} = \exp\left(\frac{Q}{RT}\right), \quad T \leq T_d \quad (50)$$

$$\log\left(\frac{\dot{\epsilon}_c}{\dot{\epsilon}_0}\right) = \frac{-a_1(T - T_s)}{a_2 + (T - T_s)}, \quad T \geq T_d \quad (51)$$

The values of the material constants $\dot{\epsilon}_{0c}$, $\dot{\epsilon}_s$, Q_c , a_1 , a_2 , T_s , T_d , σ_0 , and n_c may be found in Cheung and Cebon (1996a). The steady-state stress versus strain-rates relationship at 20°C for the bitumen tested by Cheung and Cebon is shown in Fig. 7. It can be seen from the asymptotes to the modified Cross model, the constitutive behavior can be approximated as linear viscous below $\sigma = 1 \times 10^5$ Pa and power law viscous with $n = 2.3$ above $\sigma = 1 \times 10^5$ Pa. It should be noted that for modeling purposes the bitumen is treated as a power-law viscous material with a power of 1 representing the low stress behavior and a power of 2.3 at higher stresses. No attempt is made to model the intermediate region around 10^5 Pa because the more general constitutive equation needed there [(49)] prevents use of the analysis techniques described previously.

The same bitumen tested by Cheung and Cebon was used to manufacture the idealized mixes described next.

Idealized Mixes

Four main types of mixes (in the form of cylindrical specimens) consisting of bitumen mixed with various volume fractions of different kinds of particulate inclusions were tested as follows:

1. Bitumen and 40% by volume sand particles between 300 and 600 μm .
2. Bitumen and 52% by volume sand particles between 300 and 600 μm .
3. Bitumen and 64% by volume of one of the following:
 - Spherical glass beads 1.7 mm in diameter
 - Sand particles between 300 and 600 μm
 - Sand particles between 1.18 and 2.36 mm
4. Bitumen and 75% by volume sand consisting of a mix-

ture of equal quantities of sand particles between 150 and 300 μm and 1.18 and 2.36 mm.

Two types of tests in uniaxial compression were conducted. In the constant strain rate tests, a constant displacement rate was applied to the specimen, whereas in the constant stress tests, a constant force was applied (instantaneously) to the specimen and held.

The steady-state stress versus strain rate relationship for some of the mixes at 20°C is shown in Fig. 7. It can be seen that the mix curve shows the same shape as the pure bitumen curve. The main difference between the curves is that the steady-state strain rate of the mix is less than that of pure bitumen for the same stress (i.e., the mix is stiffer than pure bitumen). The stiffening effect S is shown schematically in Fig. 7.

The stiffening effect was found to be predominantly a function of the volume fraction of the inclusions and independent of particle size and shape (the various types of inclusions in the 64% mix all gave $S \approx 1,000$). Also, tests performed at temperatures ranging from 0 to 40°C showed that the stiffening effect S was a function of the volume fraction of inclusions only, with the temperature dependency being the same as that of pure bitumen [i.e., given by (50) or (51)]. The mix with 40% by volume sand particles was only tested at 0°C because the mix was too soft to make stable compression specimens at higher temperatures. The results shown in Fig. 7 for this mix have been corrected to a temperature of 20°C using (50).

ANALYSIS

A comparison between the stiffening predicted by the analyses presented here and the experimental results for bitumen (i.e., a nonlinear viscous material with $n = 2.3$), reinforced by various volume fractions of rigid inclusions, is shown in Fig. 8. It can be seen that the predictions of the composite sphere upper-bound analysis agree well with the experimental observations over three orders of magnitude of S . Furthermore, it can be seen that Suquet's method overestimates S by about an average of 45% for the bitumen composite over the entire range of six orders of magnitude of S . However, for a random composite like asphalt, where manufacturing conditions, compositions, and microstructures greatly differ, this could be considered to be within acceptable limits. Therefore, for practical purposes it should be acceptable to use Suquet's closed-form solution to estimate the stiffening factor of subspherical rigid inclusions in a bitumen matrix.

Fig. 8 also shows that the hexagonal array analysis substantially underpredicts experimental measurements for a high volume fraction of rigid particulate inclusions. However, a com-

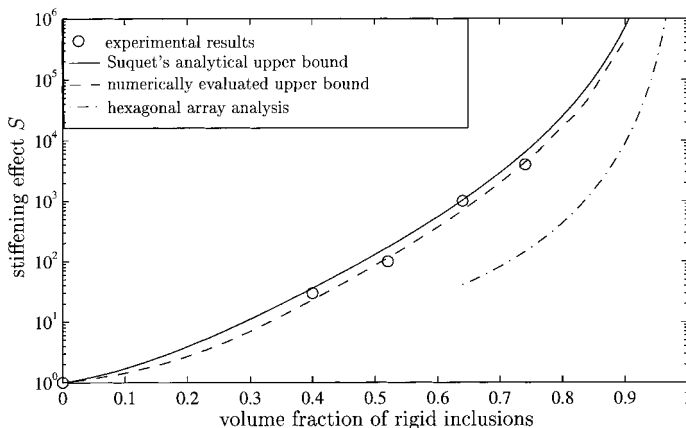


FIG. 8. Comparison between Various Models and Deshpande's (1995) Experimental Results

parison of the hexagonal array analysis with other existing models [e.g., Duva (1984), Bao et al. (1991), and lower bounds] shows that the stiffening effect predicted by this model for the regular array agrees well with that predicted by the various other analyses for the same volume fraction of rigid inclusions [see Deshpande (1995)].

Brady and Bossis (1985), using numerical calculations, and Campbell and Forgacs (1990), using percolation theory, have shown that "structure" or "cluster formation" in the aggregate is important in random or disordered composites. Analyses such as the hexagonal array analysis (i.e., analyses which give the exact solution for the stiffness of a composite with a particular known microstructure), ignore the effects of structure or clusters that form in random composites. This may be one of the reasons for the discrepancy between the predictions of the hexagonal array analysis and experimental measurements. Furthermore, the hexagonal model is a plane strain model (hence 2D). Comparisons of the predictions of this model with experimental data [three-dimensional (3D)] should thus be viewed with caution.

CONCLUSIONS

1. A simple analytical solution for the constitutive law of a regular array of rigid hexagonal prisms separated by thin films of a nonlinear viscous material under general biaxial loading was presented. The evolution of the constitutive law with compressive strain was discussed.
2. Hashin's composite sphere model was used to derive an upper-bound solution for a composite consisting of rigid inclusions in a nonlinear viscous matrix. This was evaluated numerically.
3. Suquet's closed-form, upper-bound solution for a power law viscous material reinforced by rigid particulate inclusions, obtained by transforming Hashin's linear upper bound, provides a good approximation for a composite with a matrix having a low value of the power law exponent n . However, for $n \geq 6$ Suquet's upper-bound approximation overestimates the stiffening effect substantially.
4. Hashin's composite sphere upper bound predictions of the stiffening effect S agree well with experimental measurements. However the hexagonal array analysis underestimates S by an order of magnitude.

ACKNOWLEDGMENTS

The writers would like to express their gratitude to the Cambridge Commonwealth Trust for financial support for this work.

APPENDIX. REFERENCES

- Bao, G., Hutchinson, J. W., and McMeeking, R. M. (1991). "Particle reinforcement against plastic flow and creep." *Acta Metallurgica et Materialia*, 39(8), 1871–1882.
- Brady, J. F., and Bossis, G. (1985). "The rheology of concentrated suspensions of spheres in simple shear flow by numerical simulation." *J. Fluid Mech.*, Cambridge, U.K., 155, 105–128.
- Budiansky, B., Hutchinson, J. W., and Slutsky, S. (1982). "Void growth and collapse in viscous solids." *Mechanics of solids*, H. G. Hopkins and M. J. Sewell, eds., Pergamon, Tarrytown, N.Y., 13–45.
- Campbell, G. A., and Forgacs, G. (1990). "Viscosity of concentrated suspensions: An approach based on percolation theory." *Physical Rev. A*, 41(8), 4570–4573.
- Cheung, C. Y. (1995). "The mechanical behaviour of bitumens and bituminous mixes." PhD thesis, Engrg. Dept., University of Cambridge, Cambridge, U.K.
- Cheung, C. Y., and Cebon, D. (1996a). "Experimental study of pure bitumen in tension, compression and shear." *J. Rheology*, 41(1), 45–73.
- Cheung, C. Y., and Cebon, D. (1996b). "Thin film deformation behaviour of power law creeping materials." *J. Engrg. Mech.*, ASCE, 123(11), 1138–1152.

- Cocks, A. C. F., and Ashby, M. F. (1982). "On creep fractures by void growth." *Progress in material science*, J. W. Christian, P. Haasen, and T. B. Massalski, eds., Vol. 27, Pergamon, Tarrytown, N.Y., 189–243.
- Deshpande, V. S. (1995). "Deformation behaviour of idealised bituminous mixes," Master's thesis, Engrg. Dept., University of Cambridge, Cambridge, U.K.
- Deshpande, V. S. (1997). "Steady-state deformation behaviour of bituminous mixes," PhD thesis, Engrg. Dept., University of Cambridge, Cambridge, U.K.
- Drucker, D. C. (1964). "Engineering and continuum aspects of high-strength materials." *High strength materials*, V. F. Zackay, ed., 803–813.
- Duva, J. M. (1984). "A self-consistent analysis of the stiffening effect of rigid inclusions on a power law material." *J. Engrg. Mat. and Technol.*, 106, 317–321.
- Forsythe, G. E., Malcolm, M. A., and Moler, C. B. (1977). *Computer methods for mathematical computations*. Prentice-Hall, Englewood Cliffs, N.J.
- Hashin, Z. (1962). "The elastic moduli of heterogeneous materials." *J. Appl. Mech.*, 29, 143–150.
- Hashin, Z., and Shtrikman, S. (1962). "On some variational principles in anisotropic and nonhomogeneous elasticity." *J. Mech. Phys. Solids*, 10, 335–342.
- Hervé, E., Stolz, C., and Zaoui, A. (1991). "On Hashin composite spheres assemblage." *Comptes Rendus de l'Academie des Sciences Serie II*, 313(8), 857–862.
- Hill, R. (1956). "New horizons in the mechanics of solids." *J. Mech. Phys. Solids*, 5, 66–74.
- Love, A. E. H. (1944). *A treatise on the mathematical theory of elasticity*. Dover, New York.
- Ponte Castañeda, P. (1991). "The effective mechanical properties of nonlinear isotropic composite." *J. Mech. Phys. Solids*, 39(1), 45–69.
- Ponte Castañeda, P., and Willis, J. R. (1988). "On the overall properties of nonlinearly viscous composites." *Proc., Royal Soc., London*, A416, 217–244.
- Scott, G. D., and Kilgour, D. M. (1969). "The density of random close packing of spheres." *British J. Appl. Phys.*, D2, 863–869.
- Shamo, D. F. (1970). "Conditioning of quasi-Newton methods for function minimisation." *Mathematics of Computing*, 24, 647–652.
- Sternberg, E., Eubanks, R. A., and Sadowsky, M. A. (1951). "On the axisymmetric problem of elasticity theory for a region bounded by two concentric spheres." *Proc., 1st U.S. Nat. Congr. of Appl. Mech.*, 209–215.
- Suquet, P. M. (1993). "Overall potentials and extremal surfaces of power law or ideally plastic composites." *J. Mech. Phys. Solids*, 41(6), 981–1002.
- Suquet, P. M., and Ponte Castañeda, P. (1993). "Small-contrast perturbation expansions for the effective properties of nonlinear composites." *Comptes Rendus de l'Academie des Sciences Serie II*, 317, 1515–1520.
- Talbot, D. R. S., and Willis, J. R. (1985). "Variational principles for inhomogeneous non-linear media." *J. Appl. Mathematics*, 35, 39–54.
- Whiteoak, D. (1990). *Shell bitumen handbook*. Shell Bitumen.
- Willis, J. R. (1983). "The overall elastic response of composite materials." *J. Mech. Phys. Solids*, 50, 1202–1209.
- Willis, J. R. (1989). "The structure of overall constitutive relations for a class of nonlinear composites." *J. Appl. Mathematics*, 43, 231–242.